Soils and Rocks
An International Journal of Geotechnical and Geoenvironmental Engineering
www.soilsandrocks.com
ISSN 1980-9743
ISSN-e 2675-5475

Analysis of different failure criteria to evaluate bauxite tailings mechanical behavior through numerical modelling

Giovani Jordi Bruschi[1#], Fernando Fante[1], Mariana Tonini de Araújo[1], Gustavo Dias Macedo[1], Cesar Alberto Ruver[1]

Technical Note

Keywords
Bauxite tailings
Mechanical behavior
Triaxial testing
Numerical simulation
ABAQUS

Abstract

In recent years several dam failures have been reported throughout the world, generating a social concern on mine tailings. Along these lines, it became essential to understand the mechanical behavior of these materials in order to refine current design technologies and prevent more tragedies. In this context, this research had two main goals: (i) to analyze bauxite tailings mechanical behavior through isotropically consolidated-undrained triaxial tests and consolidation tests; and (ii) to compare triaxial tests and numerical simulations results. Confining stresses of 75kPa, 150kPa, and 300kPa were applied in the triaxial tests. Numerical modelling was performed through ABAQUS software, in which three different failure criteria were analyzed, Mohr-Coulomb Model (MCM), Drucker-Prager Model (DPM), and Modified Cam-Clay Model (MCCM). Results indicated that all studied criteria showed satisfactory results, however, DPM was the best criterion to simulate bauxite tailings mechanical behavior and respective strength parameters.

1. Introduction

The mining industry generates large quantities of mine tailings daily. These materials are normally disposed of in hydraulic-fill tailing dams as slurries, and depending on their constituent minerals can negatively affect the environment if their deposition is deficient and/or incorrect (Schnaid et al., 2014). In the past decades, major incidents related to failures in mine tailing dams have been reported (Liu et al., 2015) and two recent and serious cases occurred in Brazil. The Mariana disaster, in 2015, resulted in the release of more than 50 million cubic meters of iron ore tailings, as well as in the death of 19 people (Gama et al., 2019). The Brumadinho disaster, in 2019, had more than 300 victims and 13 million cubic meters of mine tailings released (Furlan et al., 2020).

Safety assurance of mine tailing dams is a challenging task encountered in the mining process (Owen et al., 2020). The stability of these structures requires extensive geotechnical and geological investigation, such as water table configuration; aquifer boundaries; site characterization; and strength-stability analysis (Coulibaly et al., 2017). Besides, these parameters are normally associated with complex and expensive tests (e.g. SCPTu, VANE test). Numerical simulation, based on the Finite Element Method (FEM), can be presented as a relevant and low-cost alternative for predicting mine tailings strength parameters (Braga & Nogueira, 2019). The prediction of mine tailings mechanical behavior, without the need of expensive and time-demanding tests, is important in all engineering designs. In this context, ABAQUS is a software widely employed for finite element analysis in many engineering fields.

Concerning geotechnical engineering applications, Dai & Qin (2013) performed and evaluated natural clayey soil behavior using numerical simulation in ABAQUS and compared the fit between real and simulated results employing the Modified Cam-clay Model (MCCM), with simulation parameters acquired from an isotropic consolidation and triaxial tests. The model fitted well experimental e-ln p', u-ε_a, and q-ε_a curves. Grzyb et al. (2012) investigated the bearing capacity of a reinforced shallow foundation in ABAQUS, analyzing the impact of constitutive laws (Drucker-Prager and Modified Drucker-Prager with cap criteria). A small-scale laboratory model provided the simulation parameters. Results showed fair agreements among vertical force-displacement curves, measured and predicted; Drucker-Prager with cap criterion reproduced better the soil behavior. Liu & Chen (2017) implemented a strain-hardening Drucker-Prager model in ABAQUS through a subroutine, applying the numerical modeling to solve a tunnel excavation issue. Numerical results presented fair agreements with analytical ones in terms of mean effective stress, deviatoric stress, and plastic deviatoric strain. Other studies performed using ABAQUS were: (i) pipelines behavior simulation in unsaturated soils (Robert

#Corresponding author. E-mail address: giovani.bruschi@ufrgs.br
[1]Universidade Federal do Rio Grande do Sul, Departamento de Engenharia Civil, Programa de Pós-graduação em Engenharia Civil, Porto Alegre, RS, Brasil.

Submitted July 10, 2020; Final Acceptance on September 23, 2020; Discussion open until May 31, 2021.
DOI: https://doi.org/10.28927/SR.2021.053720

2017); (ii) soil-pipe interaction in dry and partially saturated sand (Jung et al. 2013); and (iii) slope stability analysis using extended Drucker-Prager yield criterion (Su and Li 2009).

However, previous works relating mine tailings and numerical analysis were performed in software other than ABAQUS. Braga & Nogueira (2019) studied a sandy tailing deposit from iron ore mining using the computational program ANLOG – Nonlinear Analysis of Geotechnical Works. Coulibaly et al. (2017) assessed the stability of a tailing dam through numerical analysis with SLOPE/W and SEEP/W. In a most recent study, Mahdi et al. (2020) numerically modeled a tailing dam containing residues of Alberta oil-sand industry in Canada by means of FLO-2D Software for two-dimensional flood or single-phase mud-flood simulation. Thus, there is a research gap related to the use of ABAQUS and tailing dams. To fill this gap, the present research sought to analyze the bauxite tailings strength behavior through isotropically consolidated-undrained triaxial testing and numerical simulation, the last performed in ABAQUS software. Three types of failure criteria were tested: Mohr-Coulomb, Drucker-Prager, and Modified Cam-Clay.

2. Experimental data

In order to obtain geomechanical parameters of the mining tailing samples, materials were collected from a bauxite mining industry in northern Brazil. Consolidated-Undrained (CIU) triaxial tests were conducted in undisturbed samples using three different confining stresses, 75kPa, 150kPa, and 300kPa. Table 1 presents the geomechanical information of each triaxial test. Terms "initial" and "final" refer to the sample's starting and ending consolidation conditions, and term "at failure" refers to peak conditions defined by the Mohr-Coulomb failure criterion. Results of the CIU triaxial tests as well as their strength parameters are shown in Figure 1 and Figure 2, respectively. In Figure 1, the p'-q plan aids on the determination of the "*M*" parameter and the critical state friction angle "ϕ_{cs}'", while the s'-t plan determines the peak friction angle "ϕ'". Schnaid et al. (2014) obtained an "*M*" value of 1.4 and a "ϕ_{cs}'" of 36° for bauxite tailings, similar to those obtained in this study.

Consolidation tests were also performed and followed ASTM D2435/D2435M-11 procedures (ASTM, 2020). Table 2 shows the parametrical information and Figure 3 shows consolidation tests graphical results.

Applying the geomechanical parameters acquired by means of experimental triaxial tests of bauxite tailing samples it was possible to perform the numerical simulations and compare computational results with experimental ones.

3. Method

The numerical analysis was based on the Finite Element Method (FEM) and performed through ABAQUS software. Three types of failure criteria were tested: Mohr-Coulomb Model (MCM), Drucker-Prager Model (DPM), and Modified Cam-Clay Model (MCCM). In ABAQUS software a 2.5 cm by 5 cm axisymmetric element was created, representing triaxial specimens with a 5 cm diameter and 10 cm height. In the model, Figure 4, the y-axis is applied to the roller to restrict horizontal movement, and the bottom horizontal surface is restricted in the vertical direction.

Table 1. Experimental triaxial data.

Parameter		σ'_3 = 75kPa	σ'_3 = 150kPa	σ'_3 = 300kPa
Initial	Height (mm)	101.0	101.2	100.5
	Diameter (mm)	48.57	50.56	49.55
	Moisture content (%)	28.4	37.0	32.3
	Dry density (N/m^3)	1.39e+4	1.28e+4	1.31e+4
	Saturation (%)	78.2	88.0	79.8
	Void ratio	1.06	1.23	1.18
Final	Moisture content (%)	35.9	40.1	36.7
	Dry density (N/m^3)	1.40e+4	1.32e+4	1.38e+4
	Cross sectional area (mm^2)	1839.0	1955.0	1832.0
	Saturation (%)	100.0	100.0	100.0
	Void ratio	1.05	1.17	1.07
	Back pressure (%)	399.0	399.0	398.9
Vertical effective consolidation stress (kPa)		74.92	153.6	300.6
Horizontal effective consolidation stress (kPa)		74.97	150.0	300.0
Vertical strain after consolidation (%)		-0.01505	-0.03742	-0.04021
Volumetric strain after consolidation (%)		0.8090	2.646	4.968
Shear strength (kPa)		58.66	92.77	117.8
Strain at failure (%)		1.58	1.85	2.32
Strain rate (%/min)		0.01247	0.01247	0.01247
Deviator stress at failure (kPa)		117.3	185.5	235.6
Effective minor principal stress at failure (kPa)		24.85	73.01	102.4
Effective major principal stress at failure (kPa)		142.2	258.5	338.0
B-Value		0.99	0.99	0.99

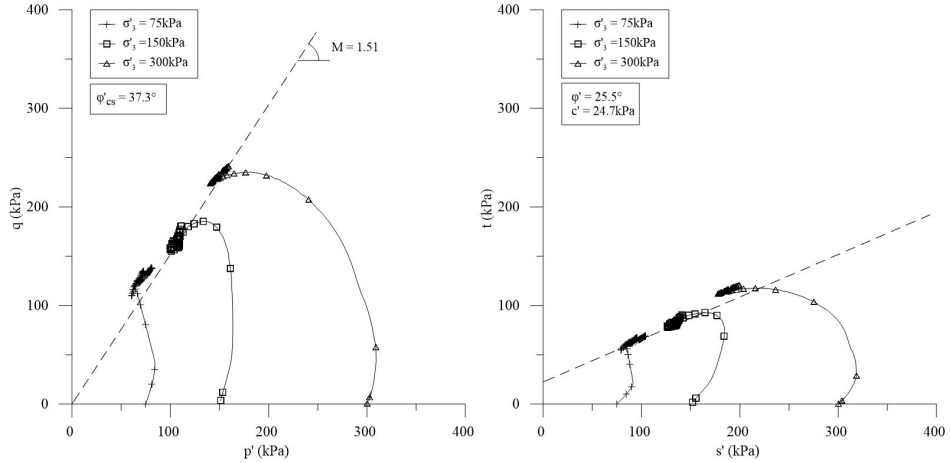

(a) (b)

Figure 1. Stress paths for the experimental triaxial data: (a) critical state parameters from p'- q plan; (b) peak parameters from s'- t plan.

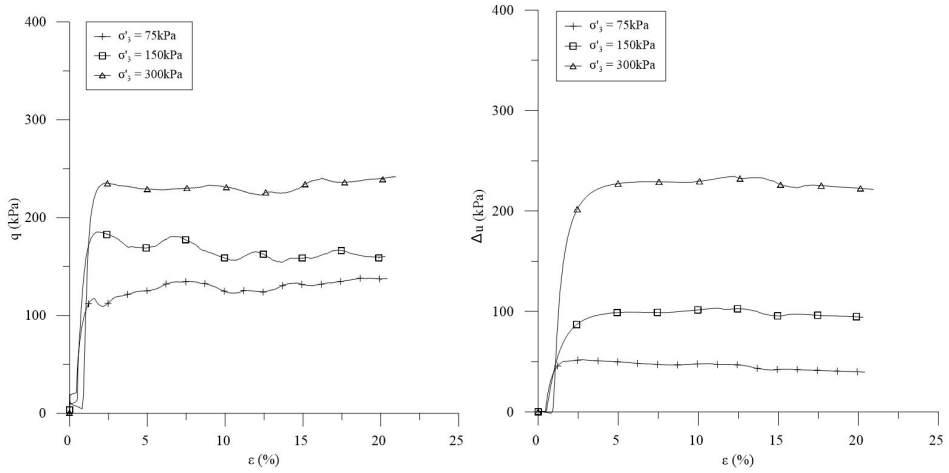

(a) (b)

Figure 2. Stress-strain curves (a) and pore-pressure variation (b) for the experimental triaxial data.

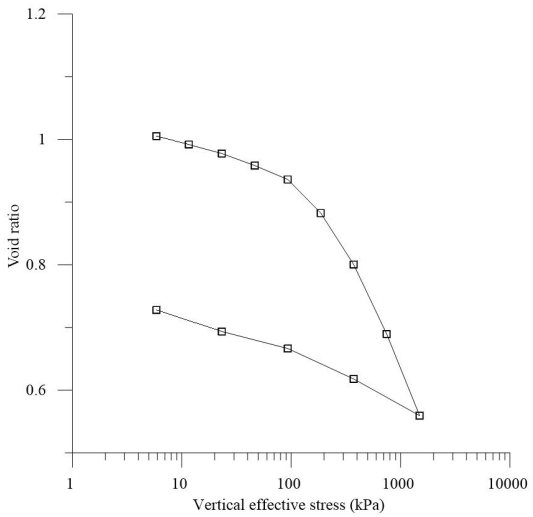

Figure 3. Isotropic consolidation test.

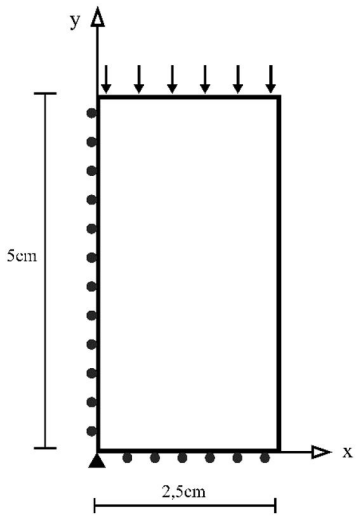

Figure 4. Numerical simulation section representation.

Table 2. Consolidation test data.

Type		Bauxite tailing
		Variegated clay
γ_n (kN/m³)		17.3
W_i (%)		36.11
W_f (%)		31.65
e_0		1.02
C_c		0.36
C_r		0.06
C_e		0.08
Λ		0.83
σ'_{vm} (kPa)		195
$e_{\sigma'vm}$		0.87
K_{20} (cm/s)	50kPa	2.67e-7
	100kPa	9.23e-8
	200kPa	3.63e-8
	400kPa	1.76e-8

Table 3. General parameters.

Confining stress - σ'_3 (kPa)	Density - ρ (kg/m³)	Permeability – k (m/s)	Specific weight of wetting liquid - γ_w (N/m³)	Voids ratio – e_0
75				1.05
150	1.36e+3	1e-9	9.81e+3	1.17
300				1.07

Table 4. MCM parameters.

Elasticity		Plasticity		
Young modulus - E (kPa)	Poisson ratio - υ	Friction angle - ϕ' (°)	Dilation angle - Ψ (°)	Cohesion intercept - c' (kPa)
0.81e+3				
1.00e+3	0.3	25.5	0	24.7
1.02e+3				

The parameters inserted in the software were divided in general (i.e. used in all failure criteria) and specific, which were subdivided in elastic and plastic for each failure criterion. The general parameters were estimated from the experimental triaxial and consolidation tests shown in Section 2 and are presented in Table 3. The density parameter was obtained by the final dry densities average (Figure 1), and permeability is a typical value for bauxite tailings (Vick, 1990). Table 4, Table 5, and Table 6 present the specific parameters for the MCM, DPM, and MCCM respectively.

For MCM parameters (Table 4), the Young Modulus (E), the peak friction angle (ϕ'), and cohesion intercept (c') were all obtained through triaxial tests experimental results. Since studied triaxial tests were CIU no volumetric strain data was available for the calculation of the dilation angle (Ψ). Thus, a value of zero was utilized for this parameter. The Poisson ratio (υ), on the other hand, was retrieved from studies on bauxite tailings (Rout et al., 2013; Wu, 2014; Feng & Yang, 2018).

On the DPM parameters (Table 5), the Young Modulus (E) and the Poisson ratio (υ) were determined in the same way as the MCM parameters. The "β" and "d" model parameters were retrieved from the peak friction angle (ϕ') and cohesion intercept (c') of the experimental triaxial tests. The cap eccentricity (R), transition surface rad, and flow stress (K) are all theoretical parameters of the DPM.

The Poisson ratio (υ) of the MCCM was determined in accordance with the procedure applied to MCM and DPM. The Log Bulk modulus (κ) and the Bulk modulus (λ) were estimated through the experimental consolidation test. The stress ratio (M) and yield surface size ($p_{0'}/2$) were retrieved from the experimental triaxial tests. Lastly, the wet yield surf. size and flow stress rate are all theoretical parameters of the MCCM.

After the MCM, DPM, and MCCM criteria were numerically simulated, stress-strain curves were plotted and analyzed. Then, strength parameters for each model were determined. The next section explores results for all studied models.

Table 5. DPM parameters.

Elasticity		Plasticity				
Young modulus (kPa) - E	Poisson ratio - υ	β (°)	d (N/m²)	Cap eccentricity - R	Transition surface rad	Flow stress - K
0.81e+3			90000			
1.00e+3	0.3	26.79	123000	0.35	0.03	1
1.02e+3			156174			

Table 6. MCCM parameters.

Elasticity		Plasticity				
Llog Bulk modulus - κ	Poisson ratio - υ	Log plas. Bulk modulus - λ	Stress ratio- M	Yield surf. Size (critical state) - $p_{0'}/2$ (N/m²)	Wet yield surf. size	Flow stress rate
0.026	0.3	0.155	1.51	1.173e+5	1	1
				1.855+5		
				2.356e+5		

4. Results and discussion

To allow verification and comparison, numerical results followed triaxial tests results representation, that is, stress-strain curves and pore-pressure variation as well as stress paths with strength parameters were drawn. Figures 5 to 7 express the stress-strain behavior and pore-pressure variation of studied failure criteria and experimental data, for each of the confining stresses, 75kPa, 150 kPa, and 300kPa. Stress paths for all models are shown in Figures 8 to 10 and strength parameters (i.e. friction angle and cohesion intercept) are presented in Table 7. It is important to note that both total and effective stress paths can be estimated through the numerical simulation, however, since experimental results were undrained tests only effective stress paths are shown in this research. Finally, results were analyzed considering (i) peak parameters – MCM and DPM; and (ii) critical state parameters – MCCM.

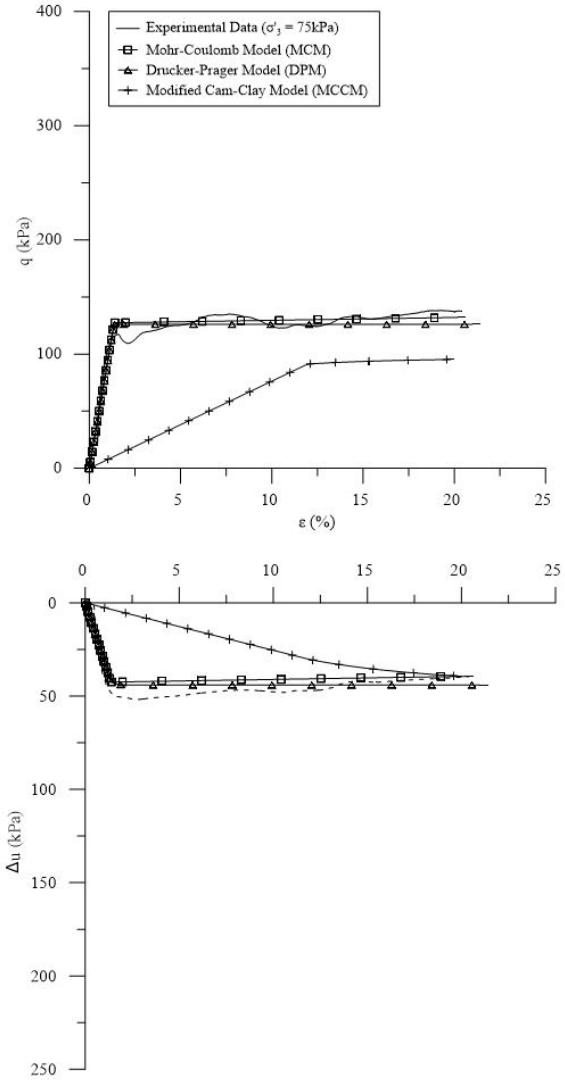

Figure 5. Simulation for 75kPa.

4.1. Peak parameters results

4.1.1. Stress-strain behavior and pore-pressure variation

It was possible to notice that in the confining stress of 75kPa the MCM accurately represented the stress-strain behavior of the bauxite tailing samples. However, on the confining stresses of 150kPa and 300kPa, the model exceeded the stress-strain of experimental results. For pore-pressure variation, MCM accurately represented the behavior on the 75kPa confining stress, and underestimated experimental results for 150kPa and 300kPa. This behavior is attributed to an elevated stress-state in conjunction with material's complexity, since this failure criterion was not created to represent materials that translate between sand and clay, such as bauxite tailings. Meanwhile, DPM accurately approached the behavior of bauxite tailings for all studied confining stresses. The model simulated stress-strain and pore-pressure variation reasonably well, presenting a small difference between numerical data and experimental results. According to Vermeer (1998), DPM presents approximate results for stiff clays with low friction angles, but not for sand, rock, or concrete.

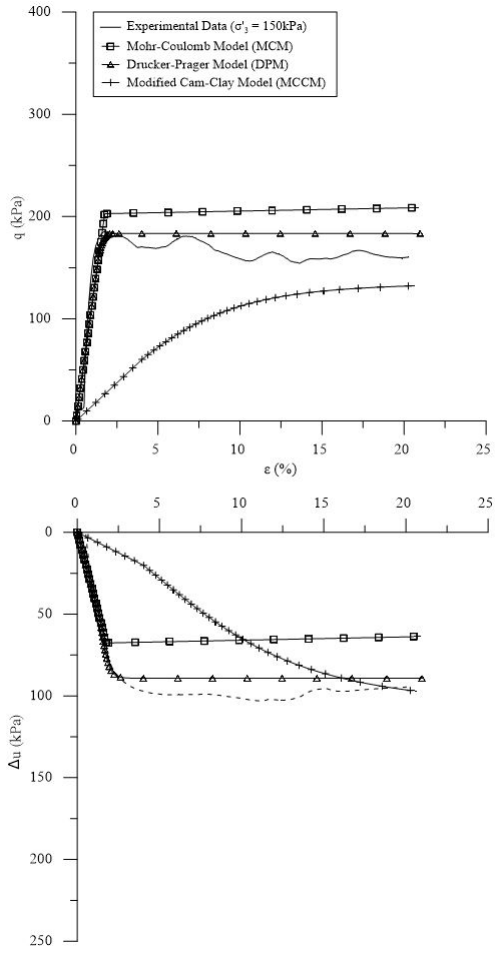

Figure 6. Simulation for 150kPa.

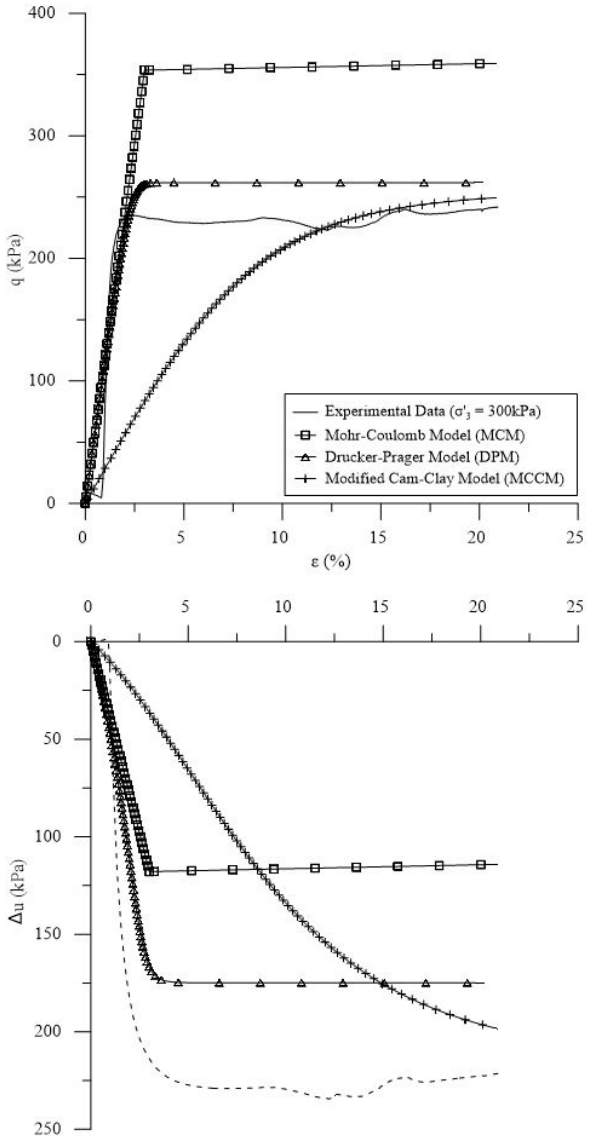

Figure 7. Simulation for 300kPa.

4.1.2. Stress paths and strength parameters

The DPM best represented stress paths and the failure envelope of bauxite tailings, presenting accurate strength parameters for all confining stresses. These results were expected, since the model was well adjusted in all numerical analyses. Although worse than DPM results, the MCM criteria presented a good estimation of the stress paths. Since strength parameters are part of the input data on the MCM, the peak friction angle and the cohesion intercept were equal to the experimental data.

4.2. Critical state parameters results

4.2.1. Stress-strain behavior and pore-pressure variation

For applied MCCM criteria, it was not possible to accurately simulate the pre-peak and peak stress-strain behavior, since the model is based on the Critical State Theory. When critical state is reached, approximately at ε=10%, the model represented fairly the material stress-strain behavior at a 300kPa confining stress. In turn, the criterion could not fully represent the stress-strain and pore-pressure variation for 75kPa and 150kPa stresses, since for these situations samples were on the overconsolidated state. In soils mechanics, the overconsolidation state or overconsolidation ratio (OCR) is the relation between the preconsolidation stress and the current soil effective stress. If OCR=1 the soil is normally

Table 7. FEM estimated strength parameters.

	Friction angle (°)	Cohesion intercept (kPa)
Experimental results (peak condition)	25.5	24.7
MCM	25.5	24.7
DPM	25.1	24.9
Experimental results (critical state condition)	37.3	0
MCCM	33.5	0

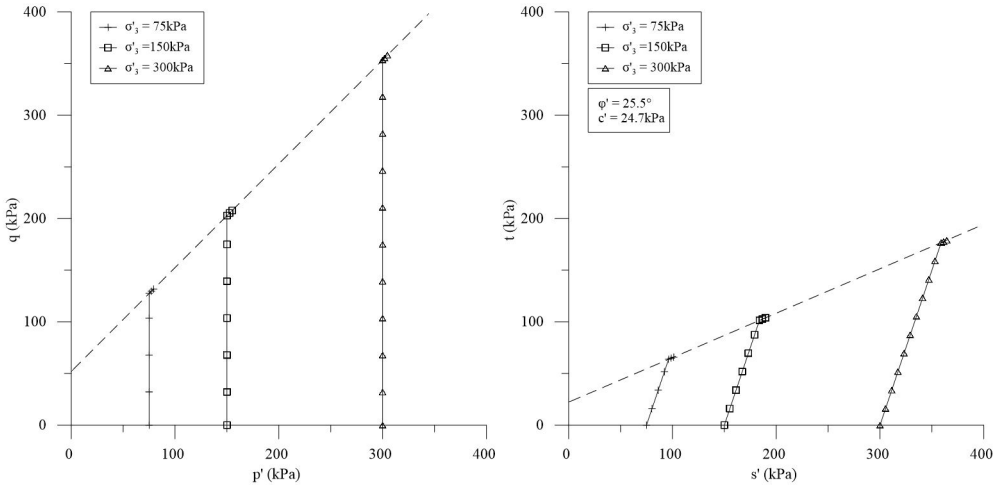

Figure 8. Stress paths MCM.

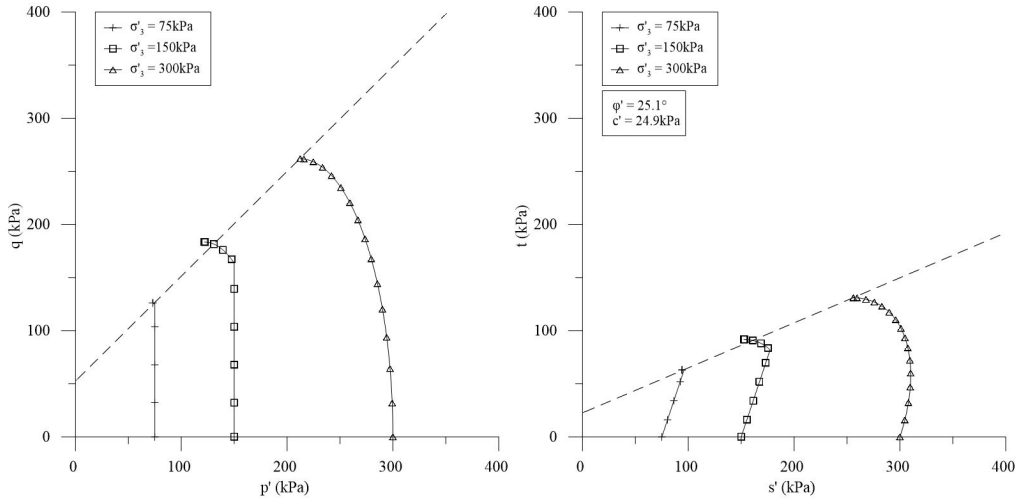

Figure 9. Stress paths DPM.

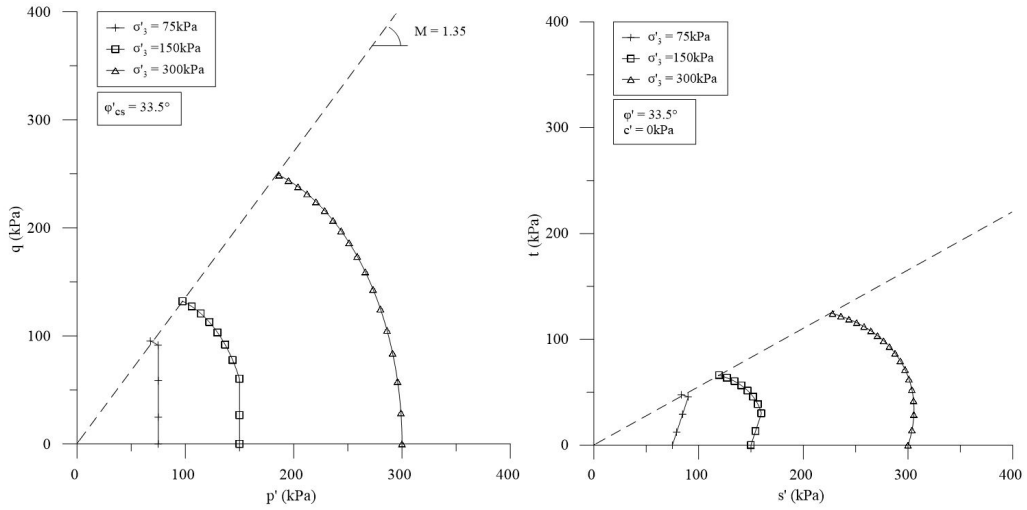

Figure 10. Stress paths MCCM.

consolidated (NC), if OCR>1 the soil is overconsolidated (OC) (Lambe & Whitman, 1979). The MCCM can simulate the mechanical behavior of normally consolidated materials satisfactorily, while it fails to predict the mechanical behavior of heavily overconsolidated soils (Fang & Daniels, 2006). One of the reasons lays on the fact that MCCM is unable to converge satisfactorily with materials that present negative variations in pore-pressure as well as softening behavior. Therefore, the model only showed good results for stresses of 300kPa (OCR=1). Likewise, the use of MCCM for simulating the mechanical behavior of overconsolidated soils can result in misleading stress-strain behavior.

4.2.2. Stress paths

In the critical state condition, the MCCM underestimated the stress paths due to samples overconsolidation. Thus, the use of this model to simulate the mechanical behavior of overconsolidated soils leads to lower strength parameters when compared to the actual strength of the materials.

5. Concluding remarks

This research presents bauxite mine tailings undrained shear strength and its mechanical behavior; then it makes a comparison between experimental and numerical triaxial tests results. The results showed that numerical simulation is a valid alternative for estimating strength parameters, as well as the mechanical behavior of bauxite tailings. The Mohr-Coulomb Model (MCM), Drucker-Prager Model (DPM), and Modified Cam-Clay Model (MCCM) were applied in the numerical analysis. Based on these experimental and theoretical results, several conclusions can be drawn and are summarized as follows:

- DPM presented the best results among all analyzed models (i.e. peak and critical parameters models), in terms of stress-strain behavior, pore pressure variation and peak strength parameters for the triaxial testing of the bauxite tailings;
- MCM served as a proper model to predict the bauxite tailings peak strength parameters. However, this

model overstated the stress-strain behavior and understated the pore pressure variation;

- MCCM bestowed satisfactory results, on the stress-strain behavior, exclusively for the normally consolidated sample (confining stress of 300kPa). This criterion failed to predict the mechanical behavior of the overconsolidated samples (confining stresses of 75kPa and 150kPa), resulting in lower strength parameters;
- Both total and effective stress paths can be estimated through numerical simulation using peak or critical state parameters, even though the experimental test was undrained;
- Results showed that numerical analysis through ABAQUS software is a valid low-cost alternative for estimating the strength parameters and the mechanical behavior of bauxite tailings. However, numerical simulation must be utilized cautiously due to the complexity and particularities of the analyzed failure criteria.

Declaration of interest

The authors certify that they have NO affiliations with or involvement in any organization or entity with any financial interest (such as honoraria; educational grants; participation in speakers' bureaus; membership, employment, consultancies, stock ownership, or other equity interest; and expert testimony or patent-licensing arrangements), or non-financial interest (such as personal or professional relationships, affiliations, knowledge or beliefs) in the subject matter or materials discussed in this manuscript.

Author's contributions

All authors contributed equally for the development of this research.

References

ASTM D2435/D2435M-11. (2020). *One-dimensional consolidation properties of soils using incremental loading*. ASTM International, West Conshohocken, PA. http://dx.doi.org/10.1520/D2435_D2435M-11R20.

Braga, A.L.C., & Nogueira, C de L. (2019). Coupled numerical simulation of a tailings deposit by fem. *Rev Esc Minas*, 72, 153-160. http://dx.doi.org/10.1590/0370-44672016720047.

Coulibaly, Y., Belem, T., & Cheng, L.Z. (2017). Numerical analysis and geophysical monitoring for stability assessment of the Northwest tailings dam at Westwood Mine. *International Journal of Mining Science and Technology*, 27, 701-710. http://dx.doi.org/10.1016/j.ijmst.2017.05.012.

Dai, Z.H., & Qin, Z.Z. (2013). Numerical and theoretical verification of modified cam-clay model and discussion on its problems. *Journal of Central South University*, 20, 3305-3313. http://dx.doi.org/10.1007/s11771-013-1854-7.

Fang, H.-Y., & Daniels, J.L. (2006). *Introductory geotechnical engineering: an environmental perspective*. CRC Press

Feng, Y., & Yang, C. (2018). Analysis on physical and mechanical properties of red mud materials and stockpile stability after dilatation. *Advances in Materials Science and Engineering*, 2018, http://dx.doi.org/10.1155/2018/8784232.

Furlan, J.P.R., dos Santos, L.D.R., Moretto, J.A.S., Ramos, M.S., Gallo, I.F.L., Alves, G.A.D., Paulelli, A.C., Rocha, C.C.S., Cesila, C.A., Gallimberti, M., Devóz, P.P., Barbosa Júnior, F., & Stehling, E.G. (2020). Occurrence and abundance of clinically relevant antimicrobial resistance genes in environmental samples after the Brumadinho dam disaster, Brazil. *The Science of the Total Environment*, 726, 138100. http://dx.doi.org/10.1016/j.scitotenv.2020.138100.

Gama, F.F., Paradella, W.R., Mura, J.C., & de Oliveira, C.G. (2019). Advanced DINSAR analysis on dam stability monitoring: a case study in the Germano mining complex (Mariana, Brazil) with SBAS and PSI techniques. *Remote Sens Appl Soc Environ*, 16, http://dx.doi.org/10.1016/j.rsase.2019.100267.

Grzyb, A., Dhaybi, M., & Pellet, F. (2012). Numerical modeling of a small scale shallow foundation reinforced by Soil-Mixing. In *Proceedings of the 2nd International Conference on Geotechnique, Construction Materials and Environment*. Kuala Lumpur – Malaysia. [CDRom].

Jung, J.K., O'Rourke, T.D., & Olson, N.A. (2013). Lateral soil-pipe interaction in dry and partially saturated sand. *Journal of Geotechnical and Geoenvironmental Engineering*, 139, 2028-2036. http://dx.doi.org/10.1061/(ASCE)GT.1943-5606.0000960.

Lambe, T.W., & Whitman, R.V. (1979). *Soil mechanics, SI version*. John Wiley & Sons, Inc.

Liu, K., & Chen, S.L. (2017). Finite element implementation of strain-hardening Drucker–Prager plasticity model with application to tunnel excavation. *Underground Space*, 2(3), 168-174. http://dx.doi.org/10.1016/j.undsp.2017.08.003.

Liu, R., Liu, J., Zhang, Z., Borthwick, A., & Zhang, K. (2015). Accidental water pollution risk analysis of mine tailings ponds in Guanting reservoir Watershed, Zhangjiakou city, China. *International Journal of Environmental Research and Public Health*, 12, 15269-15284. http://dx.doi.org/10.3390/ijerph121214983.

Mahdi, A., Shakibaeinia, A., & Dibike, Y.B. (2020). Numerical modelling of oil-sands tailings dam breach runout and overland flow. *The Science of the Total Environment*, 703, 134568. http://dx.doi.org/10.1016/j.scitotenv.2019.134568.

Owen, J.R., Kemp, D., Lèbre, É., Svobodova, K., & Pérez-Murillo, G. (2020). Catastrophic tailings dam failures and disaster risk disclosure. *International Journal of Disaster Risk Reduction*, 42, http://dx.doi.org/10.1016/j.ijdrr.2019.101361.

Robert, D.J. (2017). A modified mohr-coulomb model to simulate the behavior of pipelines in unsaturated soils.

Computers and Geotechnics, 91, 146-160. http://dx.doi.org/10.1016/j.compgeo.2017.07.004.

Rout, S.K., Sahoo, T., & Das, S.K. (2013). Design of tailing dam using red mud. *Central European Journal of Engineering*, 3, 316-328. http://dx.doi.org/10.2478/s13531-012-0056-7.

Schnaid, F., Nierwinski, H.P., Bedin, J., & Odebrecht, E. (2014). On the caracterization and classification of bauxite tailings. *Soil Rocks*, 37(2), 277-284.

Su, K., & Li, Y. (2009). Discussion of extended drucker-prager yield criterion in slope stability analysis. *Asia-Pacific Power Energy Eng Conf APPEEC*, 2, 2-5. http://dx.doi.org/10.1109/APPEEC.2009.4918285.

Vermeer, P.A. (1998). Non-associated plasticity for soils, concrete and rock. *Physics of Dry Granular Media*, 163-196.

Vick, S.G. (1990). *Planning, design, and analysis of tailings dams*. BiTech.

Wu, C.S. (2014). The drainage consolidation modeling of sand drain in red mud tailing and analysis on the change law of the pore water pressure. *Mathematical Problems in Engineering*, 2014, 876872. http://dx.doi.org/10.1155/2014/876872.

List of symbols

ASTM – American Society for Testing and Materials
CIU – Isotropically consolidated undrained
DPM – Drucker-Prager Model
FEM – Finite Element Method
MCCM – Cam-Clay Modified Model
MCM – Mohr-Coulomb Model
OCR – Over consolidation ratio
c' – cohesion intercept
Cc – coefficient of compression
Ce – coefficient of expansion
Cr – coefficient of recompression
d – MCM parameter for the cohesion intercept
e – voids ratio
E – Young modulus
e0 – initial voids ratio
$e_{\sigma'vm}$ – voids ratio at the preconsolidation stress
K – flow stress
k – permeability
M – stress ratio
p' – average effective stress
p0'/2 – Yield surface size
q – deviator stress
R – cap eccentricity
s' – (σ'1 + σ'3)/2
t – (σ'1 - σ'3)/2
wf – final water content
wi – initial water content
β – MCM parameter for the friction angle
γw – specific weight of wetting liquid
κ – Log Bulk Modulus
λ – Bulk Modulus
ϕ' – effective friction angle
Ψ – Dilation angle
Δu – porepressure variation
γn – natural unit weight
ρ − density
σ'vm – preconsolidation stress
σ'3 − confining stress
υ – Poisson ratio